Antenna Placement in a Compressive Sensing-Based Colocated MIMO Radar

Ajorloo, Abdollah; Amini, Arash; Tohidi, Ehsan; Bastani, Mohammad Hassan; Leus, Geert

Citation (APA)
Ajorloo, A., Amini, A., Tohidi, E., Bastani, M. H., & Leus, G. (2020). Antenna Placement in a Compressive Sensing-Based Colocated MIMO Radar. *IEEE Transactions on Aerospace and Electronic Systems*, *56*(6), 4606-4614. Article 9103001. https://doi.org/10.1109/TAES.2020.2998196

Important note
To cite this publication, please use the final published version (if applicable).
Please check the document version above.

Antenna Placement in a Compressive Sensing-Based Colocated MIMO Radar

ABDOLLAH AJORLOO [iD]
Sharif University of Technology, Tehran, Iran

ARASH AMINI [iD], Senior Member, IEEE
Sharif University of Technology, Tehran, Iran

EHSAN TOHIDI [iD]
Eurecom, Biot, France

MOHAMMAD HASSAN BASTANI
Sharif University of Technology, Tehran, Iran

GEERT LEUS [iD], Fellow, IEEE
Delft University of Technology, Delft, The Netherlands

Compressive sensing (CS) has been widely used in multiple-input–multiple-output (MIMO) radar in recent years. Unlike traditional MIMO radar, detection/estimation of targets in a CS-based MIMO radar is accomplished via sparse recovery. In this article, for a CS-based colocated MIMO radar with linear arrays, we attempt to improve the target detection performance by reducing the coherence of the associated sensing matrix. Our tool in reducing the coherence is the placement of the antennas across the array aperture. In particular, we choose antenna positions within a given grid. Initially, we formalize the position selection problem as finding binary weights for each of the locations. This problem is highly nonconvex and combinatorial in nature. Instead, we find continuous weight values for each location and interpret them as the probability of including an antenna at the given location. Next, we select antenna locations randomly according to the obtained probability distribution. We formulate the problem for the

general case of a MIMO radar with independent transmit and receive arrays for which we propose an iterative algorithm. For the special case of a transceiver array, the solution is obtained through a convex optimization approach. Our experiments show that the proposed method achieves a superior detection performance compared to a uniform random placement of the antennas within the array aperture.

I. INTRODUCTION

Multiple transmit (TX) and receive (RX) antennas in multiple-input–multiple-output (MIMO) radars improve the performance of the system by providing more degrees of freedom (e.g., independent transmitting waveforms) [1]–[5]. MIMO radar systems are generally divided into two categories—*widely separated* [2] and *colocated* [3]. Spatially distributed antennas in widely separated MIMO radars enable the radar to view a potential target from different angles; consequently, each transmitter–receiver pair experiences a different radar cross section. This implies spatial diversity for the radar and leads to target detection boosting. On the contrary, antennas in colocated MIMO radars are closely positioned such that all transmitter–receiver pairs view a target at nearly the same angle. An improved angular resolution, parameter identifiability, and interference rejection are the main advantages of colocated MIMO radar. In recent years, the application of compressive sensing (CS) to MIMO radar has been investigated both in the colocated case [6]–[9] and the widely separated case [10]–[12], either to reduce the overall cost and complexity (e.g., by reducing the number of TX/RX elements) or to improve the performance under the same number of antennas and measurements. In this article, by focusing on CS-based colocated MIMO radar, we investigate the placement of TX and RX antennas in linear arrays to improve the CS-based target detection and estimation performance.

Exploiting the sparsity of the scene in radar applications, CS has shown a promising performance in multitarget detection, parameter estimation, and imaging [6], [13]–[16]. The successful implementation of CS techniques for the recovery of a radar scene (for target detection/estimation) from the received noisy measurements strongly relies on two assumptions. The first is that the scene shall be sparse; that is, the number of targets should be far less than the number of possible radar cells (e.g., in the azimuth domain). This assumption is oftentimes valid [7], [8], [14]. The second is that the associated sensing matrix should be well behaved. In this regard, the restricted isometry property (RIP) [17] provides a guarantee for the recovery performance of a given sensing matrix. Although RIP is a strong sufficient condition for signal recovery, its verification for a given matrix is an NP-hard problem. Besides, in radar scenarios, the general form of the sensing matrix is mainly dictated by the physics of the problem and could be marginally controlled using design parameters such as the transmitting waveform. Therefore, the mutual coherence is a common alternative to RIP for designing or optimizing the sensing matrix [7], [18]–[21]. Since the mutual coherence somehow represents the cross correlation between the columns

of the sensing matrix, matrices with smaller coherence values suffer less from cross-column interference and usually exhibit a better performance in the recovery of sparse vectors. This translates into a better target detection performance in CS-based radars. Besides the fact that a small coherence yields some conservative bounds on the RIP order, it is feasible to evaluate the mutual coherence with a complexity that is linear in the number of compressive measurements and quadratic in the number of potential target positions.

Tuning the sensing matrix in CS-based MIMO radars through waveform design has been addressed in [7], [21]–[23] exclusively by reducing the coherence of the matrix. Aside from the waveforms, the position of the TX/RX elements is also one of the degrees of freedom of MIMO radar. The transmitting waveforms usually provide more degrees of freedom and waveform design is a more straightforward approach to improve the performance. The placement of antennas, however, could have a more dominant effect in certain settings, and in combination with waveform design could yield a substantial improvement.

In [24], given a desired radiation pattern, a method for sparse antenna placement is proposed for linear arrays (the positions of the antennas and their excitation amplitudes are obtained through the recovery of a sparse vector in a CS formulation). Dong [25] extends the work in [24] and proposes a similar method for the design of sparse planar arrays. In [26], the problem of sensor selection for source detection using planar arrays (in a CS-based framework) has been addressed through minimizing the coherence. In CS-based MIMO radar, antenna placement has been also considered in a few works such as [27] for the widely separated case and [28], [29] for the colocated case. In [27], considering a CS-based distributed MIMO radar, a greedy approach for reducing the mutual coherence is proposed to determine the antenna locations. In [28], a colocated CS-based MIMO radar is suggested with random linear arrays and Kerdock codes as the transmitting waveforms. The setting consists of M transmitters and N receivers that are independently placed within the allowed aperture $[0, \frac{MN}{2}]$ with uniform probability. Using a bound on the coherence of the resulting sensing matrix, the recovery of a certain number of targets in the range-Doppler-angle domain is guaranteed with high probability. A similar approach for antenna placement is devised in [29] for direction of arrival (DOA) estimation using a CS-based colocated MIMO radar with a reduced number of elements. Again by bounding the coherence of the resulting matrix, probabilistic uniform and nonuniform recovery guarantees are provided.

In this article, we consider the task of antenna placement for a CS-based colocated MIMO radar with linear arrays. Similar to [29], we consider the azimuth domain as the target space. For placing the antennas, we initially assume a uniform dense grid over the allowed array aperture. The grid points serve as the potential antenna locations. Then we select the locations of the antennas in a way to minimize the coherence of the resulting sensing matrix. We interpret the selection procedure as assigning binary weights to the grid points; 1 for placing an antenna and 0 for not placing an antenna. A full search for the 0/1 assignment is combinatorial in nature and not feasible in practice. Instead, we formalize the problem as assigning continuous-valued weights in [0,1] and interpret the weights as the likelihood of placing an antenna at a given grid point. We derive an optimization problem for tuning the weights for the general case of independent transmitter and receiver array antennas. This problem is not convex, yet we can devise an iterative algorithm to find a locally optimal solution. We also simplify the problem for the special case of transceiver elements (i.e., the array elements are used for both TX and RX) and obtain a convex program. In either case, the output of our method is a probability distribution for selecting the antenna locations. In numerical experiments, after obtaining the above distribution, we randomly place the antennas according to the derived probability distribution and report the average performance; it is shown that our method achieves a superior performance compared to a uniform random placement of the antennas within the aperture (as proposed by [28] and [29]).

The rest of the article is organized as follows. In Section II, we give a brief review on CS theory. In Section III, we discuss the system model. The derivation of the coherence minimization problem via antenna placement is presented in Section IV. We also present our proposed methods here. The performance analysis of the proposed methods using numerical simulations is given in Section V. Finally, Section VI concludes the article.

II. MATHEMATICAL PRELIMINARIES

Here, we provide a brief review on CS theory. Let us consider measurements of the form

$$\mathbf{y}_{M \times 1} = \mathbf{\Psi}_{M \times N} \mathbf{s}_{N \times 1} + \mathbf{n}_{M \times 1} \tag{1}$$

where $\mathbf{\Psi}$ is the sensing matrix, $\mathbf{y}$ is the measurement vector, $\mathbf{s}$ is the desired signal to be recovered, $\mathbf{n}$ is the noise vector with $\|\mathbf{n}\|_2 \leq \epsilon$ and $M < N$. The recovery of $\mathbf{s}$ from the noisy measurement vector $\mathbf{y}$ is not an easy task in general. Interestingly, under certain conditions on the sensing matrix, it is proved that the solution $\hat{\mathbf{s}}$ to the ℓ_1-minimization problem given by

$$\hat{\mathbf{s}} = \underset{\mathbf{s}}{\text{argmin}} \ \|\mathbf{s}\|_1 \quad \text{s.t.} \ \|\mathbf{y} - \mathbf{\Psi}\mathbf{s}\|_2 \leq \epsilon \tag{2}$$

approximates $\mathbf{s}$ fairly well, provided that $\mathbf{s}$ is sparse enough. When $\mathbf{s}$ has at most K nonzero entries (which is called K-sparse), one of the well-known sufficient recovery conditions on $\mathbf{\Psi}$ is the RIP of order $2K$ with $\delta_{2K} < \sqrt{2} - 1$ [17], which implies that for all $2K$-sparse vectors $\mathbf{x}$ and for $\delta_{2K} < \sqrt{2} - 1$, we have that

$$(1 - \delta_{2K})\|\mathbf{x}\|_2^2 \leq \|\mathbf{\Psi}\mathbf{x}\|_2^2 \leq (1 + \delta_{2K})\|\mathbf{x}\|_2^2. \tag{3}$$

Under this condition, the estimate $\hat{\mathbf{s}}$ of any arbitrary K-sparse vector $\mathbf{s}$ via (2) satisfies [17]

$$\|\hat{\mathbf{s}} - \mathbf{s}\|_2 < C\epsilon \tag{4}$$

where C is a constant that depends only on δ_{2K}.

As explained earlier, since verification of the RIP condition is computationally intractable in practice, it is common to assess the mutual coherence of the sensing matrix which is defined as

$$\mu(\boldsymbol{\Psi}) = \max_{i \neq j} \frac{|\boldsymbol{\psi}_i^H \boldsymbol{\psi}_j|}{\|\boldsymbol{\psi}_i\|\|\boldsymbol{\psi}_j\|} \tag{5}$$

where $\boldsymbol{\psi}_i$ represents the ith column of $\boldsymbol{\Psi}$. It is well known that a matrix $\boldsymbol{\Psi}$ (with normalized columns) with coherence $\mu(\boldsymbol{\Psi}) \leq \frac{\delta_{2K}}{2K-1}$ and $\delta_{2K} < 1$ satisfies RIP of order $2K$ [30]. Although this RIP bound is rather conservative, it is frequently observed that reducing the coherence leads to improvement of the recovery performance.

To solve the minimization problem in (2), a variety of methods including [31]–[35] are proposed in the literature. In this article, we use the Nesterov's algorithm (NESTA) proposed in [35], which besides being fast, works with complex vectors and matrices.

III. SYSTEM MODEL

We consider a MIMO radar with linear antenna arrays for transmitting and receiving. The positions of the antennas of the transmit and receive arrays are chosen from a uniform grid of positions over a predefined aperture. To model the received signals in such a MIMO radar, we first consider a hypothetical MIMO radar with extended TX and RX arrays whose elements are densely spaced at all the predefined positions in the grid. Then, we introduce sampling from these extended arrays to obtain actual arrays and derive the expression for the received signals for the actual MIMO radar using a CS formulation. We assume extended TX and RX arrays consisting of $\tilde{M}$ and $\tilde{N}$ colocated antennas, respectively. The arrays lie on the y-axis where the positions of the antennas are given by

$$\begin{aligned} y_{t,i} &= (i-1)d, \quad i = 1, \ldots, \tilde{M} \\ y_{r,j} &= (j-1)d, \quad j = 1, \ldots, \tilde{N} \end{aligned} \tag{6}$$

in which $y_{t,i}$ and $y_{r,j}$ stand for the positions of the ith TX antenna and the jth RX antenna, respectively, and d is the spacing factor (these quantities are normalized in wavelength units). The value of d shall be chosen no higher than $\frac{1}{2}$ in order to avoid ambiguities in estimating the azimuth angle of possible targets. The TX and RX arrays constitute apertures of size $L_t = (\tilde{M}-1)d$ and $L_r = (\tilde{N}-1)d$, respectively. Together, these two arrays yield a virtual MIMO array whose aperture is $L_a = L_t + L_r$. In the case of equal TX and RX apertures, we have $L_t = L_r = L_a/2$. Each antenna in the TX array transmits its dedicated waveform. Let us define the waveform matrix $\tilde{\mathbf{X}}_{L \times \tilde{M}} = [\tilde{\mathbf{x}}_1, \ldots, \tilde{\mathbf{x}}_{\tilde{M}}]$ in which $\tilde{\mathbf{x}}_i$ is the baseband signal transmitted by the ith transmitting antenna, and L is the number of signal samples in baseband. Moreover, assume there exists a target in the far-field of the radar at a specific range with DOA parameter $u = \sin\theta$ where θ is the azimuth angle (measured counter-clockwise from the array boresight). The transmit and receive steering vectors for the extended arrays at the target's DOA parameter are then, respectively, given by

$$\tilde{\mathbf{a}}(u) = \left[e^{j2\pi y_{t,1}u}, e^{j2\pi y_{t,2}u}, \ldots, e^{j2\pi y_{t,\tilde{M}}u} \right]^T \tag{7}$$

$$\tilde{\mathbf{b}}(u) = \left[e^{j2\pi y_{r,1}u}, e^{j2\pi y_{r,2}u}, \ldots, e^{j2\pi y_{r,\tilde{N}}u} \right]^T . \tag{8}$$

Now, considering the narrowband assumption, the baseband received signal at the ith receiver in the extended RX array can be written as

$$\tilde{\mathbf{r}}_i = \beta \, b_i(u)\tilde{\mathbf{X}}\tilde{\mathbf{a}}(u) + \tilde{\mathbf{n}}_i \tag{9}$$

where $\beta \in \mathbb{C}$ is the reflection coefficient of the target, $b_i(u) = e^{j2\pi y_{r,i}}$ is the ith element of $\tilde{\mathbf{b}}(u)$ (corresponding to the ith receiver), and $\tilde{\mathbf{n}}_i$ is the vector of noise samples at the ith receiver which is modeled by a circularly symmetric complex Gaussian random vector. All the received vectors $(i = 1, \ldots, \tilde{N})$ are assumed to be sent to a processing unit in which the vectors are stacked to construct the total received signal $\tilde{\mathbf{r}}$ given by

$$\tilde{\mathbf{r}} = [\tilde{\mathbf{r}}_1^T, \ldots, \tilde{\mathbf{r}}_{\tilde{N}}^T]^T = \beta \, \tilde{\mathbf{b}}(u) \otimes \tilde{\mathbf{X}}\tilde{\mathbf{a}}(u) + \tilde{\mathbf{n}} \tag{10}$$

where $\otimes$ is the Kronecker product operator and $\tilde{\mathbf{n}} = [\tilde{\mathbf{n}}_1, \ldots, \tilde{\mathbf{n}}_{\tilde{N}}]^T$ is the total noise vector. Similarly, when there exist K targets in the radar scene at $u_1, \ldots, u_K$ with corresponding reflection coefficients $\beta_1, \ldots, \beta_K$, the total received signal can be written as

$$\tilde{\mathbf{r}} = \sum_{k=1}^{K} \beta_k \, \tilde{\mathbf{b}}(u_k) \otimes \tilde{\mathbf{X}}\tilde{\mathbf{a}}(u_k) + \tilde{\mathbf{n}}. \tag{11}$$

Note that the above equation refers to a single range bin (i.e., a ring around the radar) and hence it does not include a delay. Now, let us consider the case of actual arrays which are the result of selecting some nodes from the extended arrays. In particular, we select M transmitters out of $\tilde{M}$ transmitters in the extended TX array and N receivers out of $\tilde{N}$ receivers in the extended RX array ($M < \tilde{M}$ and $N < \tilde{N}$). To model such a selection, let us define the transmitter (binary) weight vector as $\mathbf{w}_t = [w_{t,1}, \ldots, w_{t,\tilde{M}}]^T$ in which $w_{t,i}$ is a binary variable being 1 if the ith transmitter in the extended TX array is selected and zero otherwise. In a similar manner, we define the receiver weight vector as $\mathbf{w}_r = [w_{r,1}, \ldots, w_{r,\tilde{N}}]^T$. We shall have

$$\sum_{i=1}^{\tilde{M}} w_{t,i} = M, \quad \sum_{i=1}^{\tilde{N}} w_{r,i} = N. \tag{12}$$

Then, we construct a transmitter weight matrix $\mathbf{W}_t \in \{0, 1\}^{M \times \tilde{M}}$ through removing the all-zero rows of $\mathrm{diag}(\mathbf{w}_t)$ (there exist $\tilde{M} - M$ such rows in $\mathrm{diag}(\mathbf{w}_t)$). The receiver weight matrix $\mathbf{W}_r \in \{0, 1\}^{N \times \tilde{N}}$ is constructed similarly. One can inspect that

$$\begin{aligned} \mathbf{W}_t^T \mathbf{W}_t &= \mathrm{diag}\,(\mathbf{w}_t) \\ \mathbf{W}_r^T \mathbf{W}_r &= \mathrm{diag}\,(\mathbf{w}_r). \end{aligned} \tag{13}$$

Now, we can write the transmit and receive steering vectors for the actual arrays (denoted by $\mathbf{a}(u)$ and $\mathbf{b}(u)$, respectively)

as

$$\mathbf{a}(u) = \mathbf{W}_t \, \tilde{\mathbf{a}}(u)$$
$$\mathbf{b}(u) = \mathbf{W}_r \, \tilde{\mathbf{b}}(u). \tag{14}$$

Moreover, we denote the transmitting waveform matrix in this case by $\mathbf{X} \in \mathbb{C}^{L \times M}$. Then, as in (11), we can write the received vector in the actual MIMO radar as

$$\mathbf{r} = [\mathbf{r}_1^T, \ldots, \mathbf{r}_N^T]^T = \sum_{k=1}^{K} \beta_k \, \mathbf{b}(u_k) \otimes \mathbf{X}\mathbf{a}(u_k) + \mathbf{n} \tag{15}$$

where $\mathbf{n} = [\mathbf{n}_1, \ldots, \mathbf{n}_N]^T$ is the total noise vector. Now if a uniform grid of DOA parameters is available as $\gamma_1, \gamma_2, \ldots, \gamma_G$ ($G \gg K$), and it is assumed that each of the K existing targets in the scene lies approximately on one of the points of the grid, the received vector $\mathbf{r}$ can be written using a CS formulation as

$$\mathbf{r} = \boldsymbol{\Psi}\mathbf{s} + \mathbf{n} \tag{16}$$

where $\boldsymbol{\Psi} = [\mathbf{u}_1, \mathbf{u}_2, \ldots, \mathbf{u}_G]$ is the sensing matrix whose lth column (corresponding to the lth DOA γ_l) is

$$\mathbf{u}_l = \mathbf{b}(\gamma_l) \otimes \mathbf{X}\mathbf{a}(\gamma_l)$$
$$= \mathbf{W}_r \, \tilde{\mathbf{b}}(\gamma_l) \otimes \mathbf{X}\mathbf{W}_t \, \tilde{\mathbf{a}}(\gamma_l), \quad l = 1, \ldots, G \tag{17}$$

and the vector $\mathbf{s}$ is a sparse vector whose lth element (s_l) will be equal to β_k if the kth target is at the lth DOA bin (γ_l) and zero otherwise. As explained earlier, the received signal $\mathbf{r}$ in the CS formulation (16) pertains to a single range bin and we have different received signals for different range bins. So, the recovery process for detecting the possible targets is performed separately for each range bin using the received signal corresponding to that range bin (the sensing matrix is the same). Similar approaches have been adopted in works such as [21], [29], and [36].

As a special case, consider that instead of distinct transmitters and receivers, the nodes of the hypothetical MIMO radar (with the extended arrays) are transceivers. This more concretely means $y_{t,i} = y_{r,i}, \ i = 1, \ldots, \tilde{M}$. In this case, the transmitter and receiver steering vectors are the same ($\tilde{\mathbf{a}}(u) = \tilde{\mathbf{b}}(u)$) and we have just one selection vector to obtain the actual array. Hence, $\mathbf{w}_t = \mathbf{w}_r = \mathbf{w}$ and $\mathbf{W}_t = \mathbf{W}_r = \mathbf{W}$ where $\mathbf{w}$ and $\mathbf{W}$ are the transceiver weight vector and the transceiver weight matrix, respectively. Then, we have

$$\mathbf{a}(u) = \mathbf{b}(u) = \mathbf{W} \, \tilde{\mathbf{a}}(\theta) \tag{18}$$

and for $\mathbf{w}$, we also have

$$\sum_{i=1}^{\tilde{M}} w_i = M. \tag{19}$$

Under these circumstances, the lth column of the sensing matrix $\boldsymbol{\Psi}$ in (16), will become

$$\mathbf{u}_l = \mathbf{a}(\gamma_l) \otimes \mathbf{X}\mathbf{a}(\gamma_l)$$
$$= \mathbf{W}\tilde{\mathbf{a}}(\gamma_l) \otimes \mathbf{X}\mathbf{W}\tilde{\mathbf{a}}(\gamma_l). \tag{20}$$

After the recovery of $\mathbf{s}$ using a sparse recovery method (we use NESTA [35] in this article), to decide on the presence

or absence of a target in a specified DOA bin, it is enough to compare the magnitude of the corresponding element in the recovered vector $\hat{\mathbf{s}}$ by a prespecified threshold which can be determined from an acceptable probability of false alarm (P_{fa}) defined for the system.

Remark 1: In introducing the above system model, we assumed that the radar consists of ideal arrays with omnidirectional antennas. So, there would be no mutual coupling between the antenna elements. This assumption can be justified due to the fact that our final arrays are sparse (that is, the average spacing between adjacent antenna elements is a couple of times half the wavelength). Nevertheless, the effect of mutual coupling can be straightforwardly considered via incorporating mutual coupling matrices into the model (see [37] and [38] for more details).

IV. ANTENNA PLACEMENT

As explained earlier, our antenna placement is somehow based on an antenna selection from dense antenna arrays. In particular, assume that we want to place M transmitters within an aperture of size L_t and N receivers within an aperture of size L_r. This is accomplished by selecting M transmitters from an $\tilde{M}$-element extended TX array of aperture L_t and N receivers from an $\tilde{N}$-element extended RX array of aperture L_r. We carry out such a selection with the goal of coherence minimization. The general form of the problem can be stated as

$$\min_{\mathbf{w}_t, \mathbf{w}_r} \quad \mu(\boldsymbol{\Psi})$$

$$\text{s.t.} \quad \sum_{i=1}^{\tilde{M}} w_{t,i} = M, \quad \sum_{j=1}^{\tilde{N}} w_{r,j} = N$$

$$w_{t,i} \in \{0, 1\}, \ i = 1, \ldots, \tilde{M}$$
$$w_{r,j} \in \{0, 1\}, \ j = 1, \ldots, \tilde{N} \tag{21}$$

in which

$$\mu(\boldsymbol{\Psi}) = \max_{l \neq l'} \frac{|\mathbf{u}_{l'}^H \mathbf{u}_l|}{\|\mathbf{u}_{l'}\| \|\mathbf{u}_l\|} \tag{22}$$

where $\mathbf{u}_l$ is given by (17). The tunable parameters in $\mu(\boldsymbol{\Psi})$ are the weight vectors. To simplify the mutual coherence in terms of the weight vectors, we derive an expression for $\mathbf{u}_{l'}^H \mathbf{u}_l$. Note that the transmitting waveforms are known in advance for all the transmitters. As usual, we consider orthonormal waveforms $\mathbf{X}_{M \times M}$ so that $\mathbf{X}^H \mathbf{X} = \mathbf{I}$ (hence, the number of measurements in the CS expression is then MN). Further, let us denote $\mathbf{a}(\gamma_l)$ and $\mathbf{b}(\gamma_l)$ in brief by $\mathbf{a}_l$ and $\mathbf{b}_l$, respectively. Then, substituting $\mathbf{u}_l$ from (17) and using some properties of the Kronecker product gives

$$\mathbf{u}_{l'}^H \mathbf{u}_l = [\mathbf{b}_{l'} \otimes \mathbf{X}\mathbf{a}_{l'}]^H [\mathbf{b}_l \otimes \mathbf{X}\mathbf{a}_l]$$
$$= \left[\mathbf{b}_{l'}^H \otimes \mathbf{a}_{l'}^H \mathbf{X}^H \right] [\mathbf{b}_l \otimes \mathbf{X}\mathbf{a}_l]$$
$$= \left(\mathbf{b}_{l'}^H \mathbf{b}_l \right) \otimes \left(\mathbf{a}_{l'}^H \mathbf{X}^H \mathbf{X}\mathbf{a}_l \right)$$
$$= \left(\mathbf{b}_{l'}^H \mathbf{b}_l \right) \left(\mathbf{a}_{l'}^H \mathbf{a}_l \right). \tag{23}$$

Substituting $\mathbf{a}$ and $\mathbf{b}$ from (14) and using (13), we obtain

$$
\begin{aligned}
\mathbf{u}_{l'}^{H}\mathbf{u}_l &= \left(\tilde{\mathbf{b}}_{l'}^{H}\mathbf{W}_r^{H}\mathbf{W}_r\tilde{\mathbf{b}}_l\right)\left(\tilde{\mathbf{a}}_{l'}^{H}\mathbf{W}_t^{H}\mathbf{W}_t\tilde{\mathbf{a}}_l\right) \\
&= \left(\tilde{\mathbf{b}}_{l'}^{H}\operatorname{diag}\left(\mathbf{w}_r\right)\tilde{\mathbf{b}}_l\right)\left(\tilde{\mathbf{a}}_{l'}^{H}\operatorname{diag}\left(\mathbf{w}_t\right)\tilde{\mathbf{a}}_l\right).
\end{aligned}
\tag{24}
$$

Using a property of the $\operatorname{Tr}\{.\}$ operator, we can write the inner product as

$$
\mathbf{u}_{l'}^{H}\mathbf{u}_l = \operatorname{Tr}\left\{\mathbf{B}_{ll'}\operatorname{diag}\left(\mathbf{w}_r\right)\right\}\operatorname{Tr}\left\{\mathbf{A}_{ll'}\operatorname{diag}\left(\mathbf{w}_t\right)\right\}
\tag{25}
$$

where $\mathbf{A}_{ll'} = \tilde{\mathbf{a}}_l\tilde{\mathbf{a}}_{l'}^{H}$ and $\mathbf{B}_{ll'} = \tilde{\mathbf{b}}_l\tilde{\mathbf{b}}_{l'}^{H}$. Finally, the expression can be simplified as

$$
\mathbf{u}_{l'}^{H}\mathbf{u}_l = \left(\mathbf{w}_r^{T}\mathbf{b}_{ll'}\right)\left(\mathbf{w}_t^{T}\mathbf{a}_{ll'}\right)
\tag{26}
$$

where

$$
\begin{aligned}
\mathbf{a}_{ll'} &= \operatorname{diag}\left(\mathbf{A}_{ll'}\right) \\
\mathbf{b}_{ll'} &= \operatorname{diag}\left(\mathbf{B}_{ll'}\right)
\end{aligned}
\tag{27}
$$

are the vectors on the main diagonal in $\mathbf{A}_{ll'}$ and $\mathbf{B}_{ll'}$, respectively. Further, note that for $l = l'$, $\mathbf{a}_{ll} = \mathbf{b}_{ll} = \mathbf{1}$ and we have

$$
\begin{aligned}
\|\mathbf{u}_l\|^2 = \mathbf{u}_l^{H}\mathbf{u}_l &= \left(\mathbf{w}_r^{T}\mathbf{1}\right)\left(\mathbf{w}_t^{T}\mathbf{1}\right) \\
&= \left(\sum_{i=1}^{\tilde{N}}w_{r,i}\right)\left(\sum_{i=1}^{\tilde{M}}w_{t,i}\right) \\
&= MN, \quad \forall l \in \{1,\ldots,G\}.
\end{aligned}
\tag{28}
$$

Since the value of $\|\mathbf{u}_l\|$ is fixed for all l, the denominator in $\mu(\mathbf{\Psi})$ [as given by (22)] can be denied in the objective function. Also, it can be shown that for a uniform grid in the u domain, $\mathbf{a}_{ll'}$ and $\mathbf{b}_{ll'}$ merely depend on the difference between indices l, l'. Using this, one can drastically reduce the involved terms in the coherence expression in (22). Thus, the antenna selection problem can be stated as

$$
\begin{aligned}
\min_{\mathbf{w}_t,\mathbf{w}_r}\ &\max_{l=2,\ldots,G}\left|\mathbf{w}_r^{T}\mathbf{b}_{l1}\right|\left|\mathbf{w}_t^{T}\mathbf{a}_{l1}\right| \\
\text{s.t.}\ &\sum_{i=1}^{\tilde{M}}w_{t,i} = M, \quad \sum_{j=1}^{\tilde{N}}w_{r,j} = N \\
&w_{t,i} \in \{0,1\}, \quad i = 1,\ldots,\tilde{M} \\
&w_{r,j} \in \{0,1\}, \quad j = 1,\ldots,\tilde{N}
\end{aligned}
\tag{29}
$$

It is still difficult to solve the problem in (29) as the variables (i.e., the weight vectors) are binary (the search procedure is NP-hard and practically not feasible). In addition, the objective function is nonconvex. To somehow relax the problem, we allow the selection weights to be continuous-valued in $[0,1]$. Then, we have

$$
\begin{aligned}
\min_{\mathbf{w}_t,\mathbf{w}_r}\ &\max_{l=2,\ldots,G}\left|\mathbf{w}_r^{T}\mathbf{b}_{l1}\right|\left|\mathbf{w}_t^{T}\mathbf{a}_{l1}\right| \\
\text{s.t.}\ &\sum_{i=1}^{\tilde{M}}w_{t,i} = M, \quad \sum_{j=1}^{\tilde{N}}w_{r,j} = N \\
&0 \leq w_{t,i} \leq 1, \quad i = 1,\ldots,\tilde{M} \\
&0 \leq w_{r,j} \leq 1, \quad j = 1,\ldots,\tilde{N}.
\end{aligned}
\tag{30}
$$

Through the above relaxation, we can now interpret each of the continuous weight variables ($w_{t,i}$ and $w_{r,j}$) as the probability that the corresponding position in the extended array will be selected. Hence, by solving (30), we will eventually attain a nonuniform (discrete) probability distribution for the locations of the antennas within the prespecified aperture (instead of performing a hard selection). In the following, we consider two separate cases to solve (30). First, we consider the special case of transceiver nodes and then we go back to the general case of independent transmitter and receiver arrays.

A. Transceiver Nodes

In the case of transceiver elements, $\mathbf{w}_t = \mathbf{w}_r = \mathbf{w}$ and $\mathbf{a}_{ll'} = \mathbf{b}_{ll'}$ for all l and l'. So, in this case, the problem of antenna placement in (30) can be rewritten as

$$
\begin{aligned}
\min_{\mathbf{w}}\ &\max_{l=2,\ldots,G}\left|\mathbf{w}^{T}\mathbf{a}_{l1}\right|^2 \\
\text{s.t.}\ &\mathbf{1}^{T}\mathbf{w} = M, \quad \mathbf{0} \leq \mathbf{w} \leq \mathbf{1}
\end{aligned}
\tag{31}
$$

where $\mathbf{1}$ is an all-one vector of appropriate size. Note that the objective function in the above problem is convex since it is the maximum of several convex functions. Incorporating a dummy variable t, the problem in (31) can be reformulated as a second-order cone program (SOCP)

$$
\begin{aligned}
\min_{\mathbf{w},t}\ &t \\
\text{s.t.}\ &\left|\mathbf{w}^{T}\mathbf{a}_{l1}\right| \leq t, \ l = 2,\ldots,G \\
&\mathbf{1}^{T}\mathbf{w} = M, \quad \mathbf{0} \leq \mathbf{w} \leq \mathbf{1}.
\end{aligned}
\tag{32}
$$

The above SOCP (which satisfies all conditions of a convex problem) can be efficiently solved using off-the-shelve tools such as CVX, a package for specifying and solving convex programs.

B. Independent Transmitters and Receivers

Here we look at the general problem given by (30). The objective function in (30) is not convex in terms of $\mathbf{w}_t$ and $\mathbf{w}_r$. Consequently, (30) is not a convex problem and so is difficult to solve. To tackle this issue, we propose an iterative method.

Consider a situation in which the placement of the receivers is given ($\mathbf{w}_r$ is fixed) and we are only to determine $\mathbf{w}_t$. In this situation, one can replace $\left|\mathbf{w}_r^{T}\mathbf{b}_{l1}\right|$ in the objective function of (30) by a constant b_{l1} which is positive for all l. Then, the problem reduces to the problem of transmitter antenna placement which can be expressed as

$$
\begin{aligned}
\min_{\mathbf{w}_t}\ &\max_{l=2,\ldots,G}b_{l1}\left|\mathbf{w}_t^{T}\mathbf{a}_{l1}\right| \\
\text{s.t.}\ &\mathbf{1}^{T}\mathbf{w}_t = M;\ \mathbf{0} \leq \mathbf{w}_t \leq \mathbf{1}.
\end{aligned}
\tag{33}
$$

The above problem can be reformulated using the same trick as used in Section IV-A through adopting a dummy variable
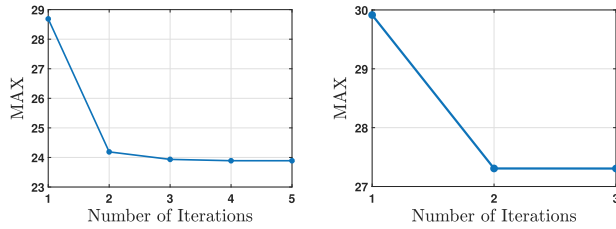
Fig. 1. Two examples of the convergence of the MAX variable in Algorithm 1.

Algorithm 1: Iterative Algorithm for Antenna Placement (Independent Transmitters and Receivers).

1: **Require:** $\{\mathbf{a}_{ll'}\}$, $\{\mathbf{b}_{ll'}\}$, M, N, and $\epsilon_1 > 0$
2: **Initialization:** $\mathbf{w}_t$ (provided that $\mathbf{1}^T \mathbf{w}_t = M$), $\text{MAX}_1 = \infty$.
3: **loop**
4:     $a_{l1} = |\mathbf{w}_t^T \mathbf{a}_{l1}|$ (for all $l = 2, \ldots, G$)
5:     Solve (35) for $\mathbf{w}_r$.
6:     Compute:
$$\text{MAX} = \max_{l=2,\ldots,G} \left|\mathbf{w}_r^T \mathbf{b}_{l1}\right| \left|\mathbf{w}_t^T \mathbf{a}_{l1}\right|$$
7:     **if** $\text{MAX}_1 - \text{MAX} < \epsilon_1$ **then**
8:       **Break**
9:     **end if**
10:     $\text{MAX}_1 \leftarrow \text{MAX}$
11:     $b_{l1} = |\mathbf{w}_r^T \mathbf{b}_{l1}|$ (for all $l = 2, \ldots, G$)
12:     Solve (34) for $\mathbf{w}_t$.
13:     go to line #6.
14: **end loop**
15: **Output:** $\mathbf{w}_t$, $\mathbf{w}_r$.

---

leading to

$$\min_{\mathbf{w}_t, t} \quad t$$
$$\text{s.t.} \quad b_{l1} \left|\mathbf{w}_t^T \mathbf{a}_{l1}\right| < t, \quad l = 2, \ldots, G$$
$$\mathbf{1}^T \mathbf{w}_t = M, \quad \mathbf{0} \leq \mathbf{w}_t \leq \mathbf{1}. \quad (34)$$

Similarly, consider the case where $\mathbf{w}_t$ is given. Then, through replacing $|\mathbf{w}_t^T \mathbf{a}_{l1}|$ by a constant a_{l1} in the objective function, we can formulate the problem of receiver antenna placement as

$$\min_{\mathbf{w}_r, t} \quad t$$
$$\text{s.t.} \quad a_{l1} \left|\mathbf{w}_r^T \mathbf{b}_{l1}\right| < t, \quad l = 2, \ldots, G$$
$$\mathbf{1}^T \mathbf{w}_r = N, \quad \mathbf{0} \leq \mathbf{w}_r \leq \mathbf{1}. \quad (35)$$

The problems of transmitter and receiver placement represented by (34) and (35), respectively, are both SOCPs and can be solved using CVX. So, our idea is to iterate between solving (34) and (35) until convergence. The details of this iterative method are given in Algorithm 1.

Note that the proposed iterative scheme ensures a reduction of the coherence in each of its iterations and hence guarantees the convergence to a local minimum.

We found in our experiments that the above algorithm converges in very few iterations. To illustrate, the convergence of the algorithm is shown in Fig. 1 for two different setups.

V. PERFORMANCE ANALYSIS

In this section, we consider equal TX and RX apertures ($L_t = L_r$). The size of the virtual aperture is therefore $L_a = 2L_t$. The potential resolution reached by such an aperture is equal to $1/L_a$. Accordingly, we adopt a uniform grid of $1/L_a$-spaced DOA parameters ($\gamma_1, \gamma_2, \ldots, \gamma_G$) in the interval $[-1 + \frac{1}{L_a}, 1]$ (the number of grid points will be $G = 2L_a$). Note that in the recovery guarantees given in [29], however, the resolution of the grid has been set to $2/L_a$. We give the results for both considered cases—transceiver elements and independent transmitter and receiver elements. In the following simulations, we choose $L_a = 100$ and $d = 1/2$, which means the number of elements in the extended arrays is $\tilde{M} = \tilde{N} = 101$. For different values of $M = N$, we obtain antenna location probability distributions in the case of transceiver elements through optimizing $\mathbf{w}$ by solving (32) using CVX. We do the same for the case of independent transmitters and receivers through obtaining $\mathbf{w}_t$ and $\mathbf{w}_r$ from Algorithm. 1. In the initialization step of the algorithm, we choose the weight vector at random. The resulting antenna location probabilities across the array (on the y-axis) for some values of M in both cases are shown in Figs. 2 and Fig. 3. As can be seen, for smaller values of M, the proposed methods assign larger weights to the ends of the arrays in order to extend the array aperture (or equivalently narrow the main beam). However, as M increases, we see that the weights in the middle of the arrays also begin to increase. Moreover, as expected, it is seen that the obtained values are symmetric around the center of the arrays. This can be understood from the symmetry in the DOA grid and the extended array structures. To analyze the achieved coherence values, for each value of M, we take 2000 independent feasible samples (2000 independent placements) from the obtained probability distributions. Note that some samples are not feasible since they do not satisfy (12) or (19). We also produce 2000 independent placements by choosing the positions uniformly at random in the interval $[0, L_t]$ (the placement method proposed by [28] and [29]). We call our proposed antenna placement method PAP and the random antenna placement RAP. We depict the achieved average coherence values in Fig. 4. As it is seen, our PAP achieves lower coherence values than the RAP for both cases. For larger values of M, our PAP for the case of transceivers achieves even lower values than the RAP for the independent transmitter/receiver case. The results shown in Fig. 4 are important as they can be used to decide on how many antennas to be employed. Such a decision should be made according to the expected number of targets (expected sparsity level). Although it is obvious that an increase in the number of antennas raises the chance of recovering more targets (due to reduction in coherence), it is not straightforward to
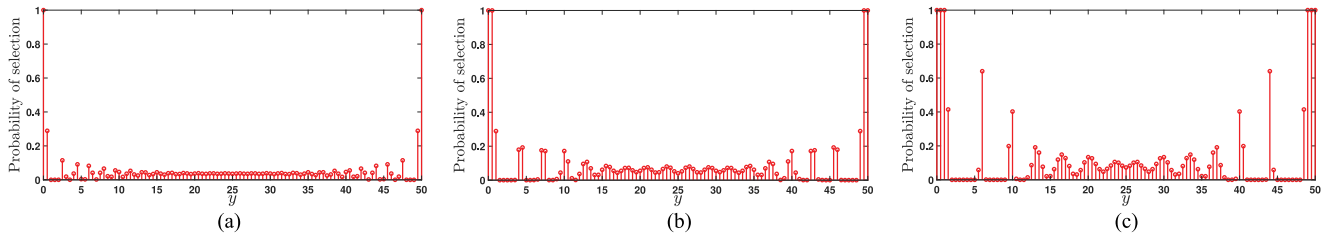
Fig. 2. Antenna placement probabilities across the array aperture on the y-axis in the case of transceiver elements. y-axis is normalized to wavelength units. (a) M = 6. (b) M = 10. (c) M = 19.
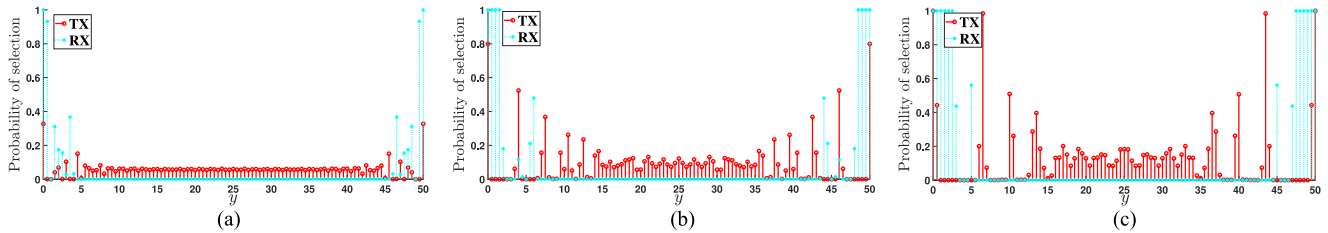

Fig. 3. Antenna placement probabilities across the array aperture on the y-axis in the case of independent transmitters and receivers. y-axis is normalized to wavelength units. (a) M = 6. (b) M = 10. (c) M = 19.
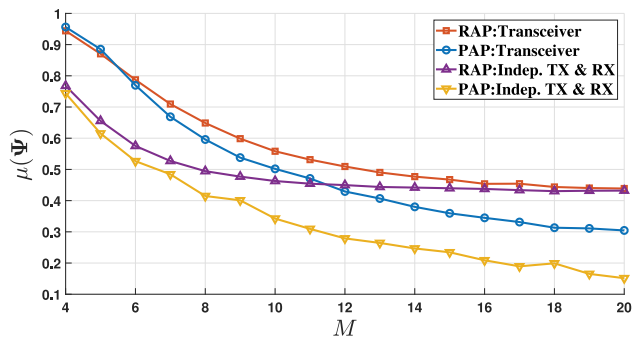

Fig. 4. Average coherence values obtained using our proposed antenna placement method and a (uniformly) random antenna placement.

specify a certain relation between the number of antennas and the guaranteed number of targets that can be detected. In such a situation, we can use the Monte Carlo simulations which generate performance curves under certain settings.

To evaluate the CS-based multitarget detection performance of the proposed method, we generate power curves (curves of probability of detection P_d versus SNR for a fixed probability of false alarm P_{fa}). To this end, we conduct a Monte Carlo simulation using 10 000 independent realizations of antenna positions, noise, target locations, and gains. In addition, we use orthogonal monotone signals for the transmitting waveforms; in particular, we consider an $M \times M$ DFT matrix as the waveform matrix $\mathbf{X}$. In each trial, we produce $K = 3$ targets located randomly on the grid points with random reflection coefficients (β_ks) following a swerling case I model [39]. That is, the β_ks follow a standard complex Gaussian distribution ($|\beta_k|$ is Rayleigh distributed with $E\{|\beta_k|^2\} = 1$)). Then, we construct the noisy

measurements using the CS expression (16) and attempt to recover the target scene (or the vector $\mathbf{s}$) using NESTA [35]. Next, we compare each of the recovered values with a threshold to declare if there is a target at the corresponding DOA or not. The threshold value is determined using the value of P_{fa} which we set to 10^{-4}. Note that the P_{fa} equals the number of target declarations on the grid points where there are not actually any targets, divided by the total number of such points (here we have $197 \times 10\,000$ such points). Finally, we compute P_d by dividing the number of exact detections by the total number of targets which is $3 \times 10\,000$ in this case. We repeat the above procedure for different SNR values (defined as $1/\sigma^2$ where σ^2 is the power of the complex Gaussian noise at the receivers). We have plotted the power curves for $M = 10$ and $M = 14$ for different methods in Fig. 5. As expected, in both cases, our PAP consistently achieves a higher probability of detection as compared with RAP. Another expected observation is that distinct arrays for transmitting and receiving exhibit superior performance compared to a transceiver array; this superior performance is of course at the penalty of increasing the total cost.

As a last experiment, we examine the effect of the number of targets in the performance of the CS-based target detection. Similar to the previous experiment, using a Monte Carlo simulation, we obtain the probability of detection for different values of K (the number of targets) while fixing P_{fa} and SNR. The results are shown in Fig. 6(a) for $M = 10$, SNR = 8dB, and $P_{fa} = 10^{-4}$ and in Fig. 6(b) for $M = 14$, SNR = 2dB, and $P_{fa} = 10^{-4}$ which again show the consistent superiority of our PAP schemes over their RAP counterparts. It should be mentioned that in obtaining the curves in Fig. 6, 10 000 independent runs have been executed for each point.
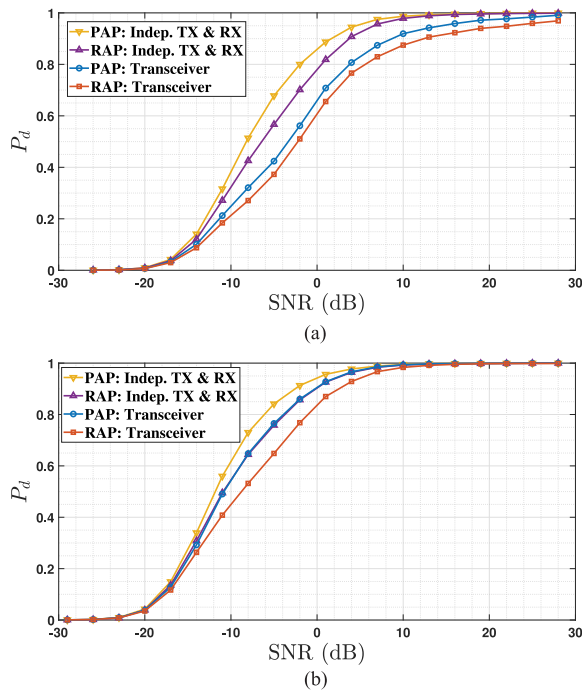
Fig. 5. CS-based detection power curves for different antenna placement methods, $K = 3$, $P_{fa} = 10^{-4}$. (a) M = 10. (b) M = 14.

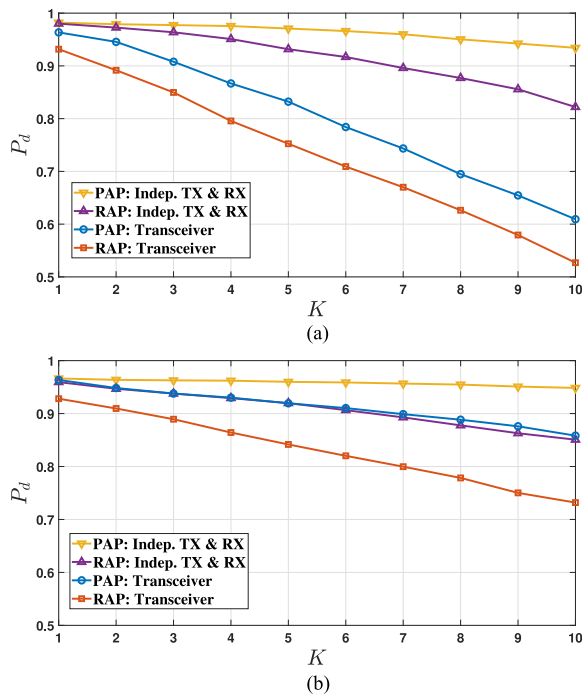Fig. 6. Probability of detection versus number of targets. (a) $M = 10$, SNR = 8dB, $P_{fa} = 10^{-4}$ (b) $M = 14$, SNR = 2dB, $P_{fa} = 10^{-4}$.

VI. CONCLUSION

An antenna placement scheme for a CS-based colocated MIMO radar was proposed in this article. Our approach is based on minimizing the coherence of the sensing matrix so as to improve the CS-based (multiple) target detection performance of the resulting MIMO array in the DOA

domain. In particular, we modeled the antenna placement as an antenna selection from extended dense arrays; using continuous weights (instead of binary ones), we developed a soft selection framework where the output is the probability of selection of antennas across the array. To solve for the weight vectors, we derived the coherence minimization problem for two cases—a MIMO radar with independent TX and RX elements, and a MIMO radar with transceiver elements. An iterative algorithm which iterates between the placement of transmitters and receivers was proposed for the former. However, for the latter, we obtained the solution using convex optimization. Our experiments showed that our proposed probability distributions achieve lower coherence values and consequently better detection performance compared to random linear arrays proposed by existing works.

REFERENCES

[1] E. Fishler, A. Haimovich, R. Blum, D. Chizhik, L. Cimini, and R. Valenzuela
     MIMO radar: An idea whose time has come
     In *Proc. IEEE Radar Conf.*, 2004, pp. 71–78.
[2] A. M. Haimovich, R. S. Blum, and L. J. Cimini
     MIMO radar with widely separated antennas
     IEEE Signal Process. Mag., vol. 25, no. 1, pp. 116–129, Jan. 2008.
[3] J. Li and P. Stoica
     MIMO radar with colocated antennas
     IEEE Signal Process. Mag., vol. 24, no. 5, pp. 106–114, Sep. 2007.
[4] B. Friedlander
     Waveform design for MIMO radars
     IEEE Trans. Aerosp. Electron. Syst., vol. 43, no. 3, pp. 1227–1238, Jul. 2007.
[5] E. Tohidi, M. Coutino, S. P. Chepuri, H. Behroozi, M. M. Nayebi, and G. Leus
     Sparse antenna and pulse placement for colocated MIMO radar
     IEEE Trans. Signal Process., vol. 67, no. 3, pp. 579–593, Feb. 2019.
[6] Y. Yu, A. P. Petropulu, and H. V. Poor
     MIMO radar using compressive sampling
     IEEE J. Sel. Topics Signal Process., vol. 4, no. 1, pp. 146–163, Feb. 2010.
[7] C.-Y. Chen and P. Vaidyanathan
     Compressed sensing in MIMO radar
     In *Proc. 42nd Asilomar Conf. Signals, Syst. Comput.*, 2008, pp. 41–44.
[8] T. Strohmer and B. Friedlander
     Analysis of sparse MIMO radar
     Appl. Comput. Harmon. Anal., vol. 37, no. 3, pp. 361–388, 2014.
[9] Y. Yu, A. P. Petropulu, and H. V. Poor
     CSSF MIMO radar: Compressive-sensing and step-frequency based MIMO radar
     IEEE Trans. Aerosp. Electron. Syst., vol. 48, no. 2, pp. 1490–1504, Apr. 2012.
[10] S. Gogineni and A. Nehorai
     Target estimation using sparse modeling for distributed MIMO radar
     IEEE Trans. Signal Process., vol. 59, no. 11, pp. 5315–5325, Nov. 2011.
[11] B. Li and A. P. Petropulu
     Distributed MIMO radar based on sparse sensing: Analysis and efficient implementation
     IEEE Trans. Aerosp. Electron. Syst., vol. 51, no. 4, pp. 3055–3070, Oct. 2015.

[12] E. Tohidi, M. Radmard, M. N. Majd, H. Behroozi, and M. M. Nayebi
Compressive sensing MTI processing in distributed MIMO radars
IET Signal Process., vol. 12, no. 3, pp. 327–334, May_2018.

[13] M. A. Herman and T. Strohmer
High-resolution radar via compressed sensing
IEEE Trans. Signal Process., vol. 57, no. 6, pp. 2275–2284, Jun. 2009.

[14] J. H. Ender
On compressive sensing applied to radar
Signal Process., vol. 90, no. 5, pp. 1402–1414, 2010.

[15] L. C. Potter, E. Ertin, J. T. Parker, and M. Cetin
Sparsity and compressed sensing in radar imaging
Proc. IEEE, vol. 98, no. 6, pp. 1006–1020, Jun. 2010.

[16] G. Han, L. Wan, L. Shu, and N. Feng
Two novel DOA estimation approaches for real-time assistant calibration systems in future vehicle industrial
IEEE Syst. J., vol. 11, no. 3, pp. 1361–1372, Sep. 2017.

[17] E. J. Candes
The restricted isometry property and its implications for compressed sensing
Comptes Rendus Mathematique, vol. 346, nos. 9–10, pp. 589–592, 2008.

[18] J. Zhang, D. Zhu, and G. Zhang
Adaptive compressed sensing radar oriented toward cognitive detection in dynamic sparse target scene
IEEE Trans. Signal Process., vol. 60, no. 4, pp. 1718–1729, Apr. 2012.

[19] H. Hu, M. Soltanalian, P. Stoica, and X. Zhu
Locating the few: Sparsity-aware waveform design for active radar
IEEE Trans. Signal Process., vol. 65, no. 3, pp. 651–662, Feb. 2017.

[20] A. Ajorloo, A. Amini, and M. H. Bastani
An approach to power allocation in MIMO radar with sparse modeling for coherence minimization
In *Proc. 25th Eur. Signal Process. Conf.*, 2017, pp. 1927–1931.

[21] Y. Yu, S. Sun, R. N. Madan, and A. Petropulu
Power allocation and waveform design for the compressive sensing based MIMO radar
IEEE Trans. Aerosp. Electron. Syst., vol. 50, no. 2, pp. 898–909, Apr. 2014.

[22] S. Gogineni and A. Nehorai
Frequency-hopping code design for MIMO radar estimation using sparse modeling
IEEE Trans. Signal Process., vol. 60, no. 6, pp. 3022–3035, Jun. 2012.

[23] A. Ajorloo, A. Amini, and M. H. Bastani
A compressive sensing based colocated MIMO radar power allocation and waveform design
IEEE Sensors J., vol. 18, no. 22, pp. 9420–9429, Nov. 2018.

[24] L. Li, W. Zhang, and F. Li
The design of sparse antenna array
2008, *arXiv:0811.0705*.

[25] X. Dong
Design of sparse antenna array with compressive sensing
Ph.D. dissertation, School of Eng., Comput. Math. Sci., Auckland Univ. Technol., Auckland, New Zealand, 2018.

[26] A. Ajorloo, R. Amiri, M. Bastani, and A. Amini
Sensor selection for sparse source detection in planar arrays
Electron. Lett., vol. 55, no. 7, pp. 411–413, 2019.

[27] P. Chen, C. Qi, and L. Wu
Antenna placement optimisation for compressed sensing-based distributed MIMO radar
IET Radar, Sonar Navigation, vol. 11, no. 2, pp. 285–293, 2017.

[28] T. Strohmer and H. Wang
Accurate imaging of moving targets via random sensor arrays and Kerdock codes
Inverse Problems, vol. 29, no. 8, 2013, Art. no. 085001.

[29] M. Rossi, A. M. Haimovich, and Y. C. Eldar
Spatial compressive sensing for MIMO radar
IEEE Trans. Signal Process., vol. 62, no. 2, pp. 419–430, Jan. 2014.

[30] S. Foucart and H. Rauhut
An invitation to compressive sensing
in *A Mathematical Introduction to Compressive Sensing*. Berlin, Germany: Springer, 2013, pp. 1–39.

[31] S. S. Chen, D. L. Donoho, and M. A. Saunders
Atomic decomposition by basis pursuit
SIAM Rev., vol. 43, no. 1, pp. 129–159, 2001.

[32] J. A. Tropp and A. C. Gilbert
Signal recovery from random measurements via orthogonal matching pursuit
IEEE Trans. Inf. Theory, vol. 53, no. 12, pp. 4655–4666, Dec. 2007.

[33] E. Candes and T. Tao
The Dantzig selector: Statistical estimation when p is much larger than n
Ann. Statist., pp. 2313–2351, 2007.

[34] H. Mohimani, M. Babaie-Zadeh, and C. Jutten
A fast approach for overcomplete sparse decomposition based on smoothed ℓ^0 norm
IEEE Trans. Signal Process., vol. 57, no. 1, pp. 289–301, Jan. 2009.

[35] S. Becker, J. Bobin, and E. J. Candès
NESTA: A fast and accurate first-order method for sparse recovery
SIAM J. Imag. Sci., vol. 4, no. 1, pp. 1–39, 2011.

[36] I. Bekkerman and J. Tabrikian
Target detection and localization using MIMO radars and Sonars
IEEE Trans. Signal Process., vol. 54, no. 10, pp. 3873–3883, Oct. 2006.

[37] C. Zhang, H. Huang, and B. Liao
Direction finding in MIMO radar with unknown mutual coupling
IEEE Access, vol. 5, pp. 4439–4447, 2017.

[38] P. Chen, Z. Cao, Z. Chen, and X. Wang
Off-grid DOA estimation using sparse Bayesian learning in MIMO radar with unknown mutual coupling
IEEE Trans. Signal Process., vol. 67, no. 1, pp. 208–220, Jan. 2018.

[39] M. I. Skolnik
Introduction to Radar Systems, 3rd ed. New York, NY, USA: McGraw Hill, 2001.